Applied Physics Letters ARTICLE pubs.aip.org/aip/apl

Parallel manipulation of multiple ink droplets via near-infrared light on lubricant infused surface

Cite as: Appl. Phys. Lett. **126**, 021602 (2025); doi: 10.1063/5.0241263
Submitted: 29 September 2024 · Accepted: 23 December 2024 ·
Published Online: 13 January 2025

Yalin Hu,[1] Jie Wu,[1] Haiyan Luo,[1] Guanqi Su,[2] Xiangxi Meng,[3] Liyu Liu,[1] and Guo Chen[1,a)]

AFFILIATIONS

[1]Chongqing Key Laboratory of Interface Physics in Energy Conversion, College of Physics, Chongqing University, Chongqing 401331, China
[2]Chongqing BI Academy, Chongqing 401120, China
[3]Shenzhen College of International Education, Shenzhen 518043, China

[a)]Author to whom correspondence should be addressed: wezer@cqu.edu.cn

ABSTRACT

Previous studies on light-driven droplet transport often use light to heat the substrate to generate a temperature difference, thereby changing the wettability or surface tension at two ends of a droplet, to propel the droplet forward, and not much attention has been paid to the droplets with photothermal properties. Herein, we introduce a method of ink droplet manipulation via near infrared light-driven on lubricant infused surfaces. Rather than heating the substrate itself, this method uses near-infrared light to irradiate one end of an ink droplet, creating a temperature gradient inside it and forming a Marangoni flow that pushes the droplet forward. It is demonstrated that the ink droplets would experience two stages during sliding, and the movement ability of the ink droplets depends on their absorbance and size; specifically, the average acceleration and steady velocity of the droplets are both positively correlated with their absorbance and negatively correlated with their volume. The work not only proves that the method can realize conventional individual droplet manipulation such as controllable transport along arbitrary paths, but also proposes a unique customized transport and merging strategy for multiple ink droplets. This investigation offers a simple and versatile manipulation approach for ink droplets, and the relevant results have potential applications in the fields of precise maneuver of light-driven droplets and droplet-based inkjet printing.

Droplet manipulation has been widely concerned because of its important applications, in which the controllable transport of droplets is one of the research hotspots.[1,2] Various strategies for droplets transport draw inspiration from natural biological structures, such as the biomimetic and efficient water collection chips inspired by cactus spine, the bioinspired chips capable of spontaneous and directional droplet transportation by synergistically combining geometric asymmetry and surface super-hydrophilicity,[3] the directional water collection artificial fiber designed to imitate the periodic spindle knots of spider silk,[4] and the intelligent fluid control interface inspired by the flexible nano tips and the overlapping micro scales arranged in directions on the wings of butterflies.[5] In addition to these, a variety of bionic functional surfaces for directional transport of droplets have also been successfully developed.[6–17]

Droplets tend to move toward areas with a higher wettability, but due to the limited range of surface wetting gradient force, it is difficult to achieve efficient droplet transport over long distances.[18–24] Therefore, scientists proposed to use external fields to assist the directional transport of droplets, including but not limited to magnetic driven,[25–27] electric driven,[28,29] optical driven,[30,31] and photothermal driven.[32,33] It is worth noting that lubricant-infused surface (LIS) has emerged as a new and remarkable type of surface since the pioneering work of Ref. 34. Chemically homogeneous lubricant with low surface energy and mobility makes LIS defect-free, spontaneously smooth, and repellant, allowing droplets to achieve an extremely low contact angle hysteresis.[35] In addition, most of the droplets transported on LIS are common pure droplets such as deionized water or ethanol, and little attention has been paid to the composite droplets such as magnetic droplets, photothermal droplets, and ink droplets. The precise manipulation of ink droplets has very important application value in droplet inkjet printing and textile printing, but there is little related research work, which is worthy of further exploration.

In this work, ink droplets with inherent photothermal properties can directly generate heat from the light, eliminating the need for an additional photothermal layer. This simplifies the substrate structure and is eco-friendly. Compared to the method driven by the surface

temperature gradient, this direct driving of droplets by near-infrared light (NIR) can achieve more precise manipulation. Our experimental results show that different colored ink droplets have different absorbances, and the ability of the droplets to move depends on the absorbance and size of the droplets. By moving the irradiation position of the NIR, the ink droplets can not only travel in a straight line, but also follow a variety of curved paths. Furthermore, by controlling the irradiated area of near-infrared light, it is also possible to realize customized merging of ink droplets of various sizes and colors.

The schematic diagram of substrate preparation is shown in Fig. 1(a), and more details can be found in the supplemental material. Numerous micropores are formed inside the silica nanoparticle layer sprayed on the quartz glass substrate, as shown in the scanning electron microscope (SEM) image of Fig. 1(b). The porous structure makes the surface superhydrophobic, which also provides conditions for the storage and retention of lubricant. Silicone oil was chosen as the lubricant, and the prepared surface is called silicon based porous sliding surface (SPSS). The silicone oil layer on the SPSS facilitates the manipulation of the light-driven droplets. The NIR laser with uniform intensity irradiates straight down to one end of the droplet and heats it up, driving the droplet forward, and the laser is moved with the droplet in the experiment. If the ink droplet is replaced with a pure deionized water droplet, no obvious temperature change and droplet movement can be observed, which indicates that the composition of the ink droplet plays a key role in the droplet movement. The principle of photothermal driven ink droplets is that the local heating of the ink droplet generates a temperature gradient between the two ends of the droplet, which leads to the formation of a gradient in the surface tension of the droplet at the droplet–air interface and generates a Marangoni flow [Fig. 1(c)], the liquid inside the droplet flows through the top of the droplet from the heated side to the unheated side, while the liquid in contact with the base flows in the opposite direction, and the two flows constitute a closed cycle inside the droplet. Figure 1(d) shows the four different colors of ink used in the experiment, which are black, blue black, blue, and red. The absorbances of the four colors of ink in the near infrared band are shown in Fig. 1(e). Black ink has the strongest absorbance, which is about 2, 3, and 5 orders of magnitude stronger than blue black, blue, and red ink, respectively. The temperature curve of light irradiated inks with time measured by infrared thermometer can also reflect the difference of light absorption capacity of different colored inks. The darker the color of the ink, the stronger the absorption ability, the faster its heating rate. Figure 1(f) shows the temperature measurement results of ink droplets fixed on the glass sheet under near-infrared light, which can be seen that black ink is quickly heated

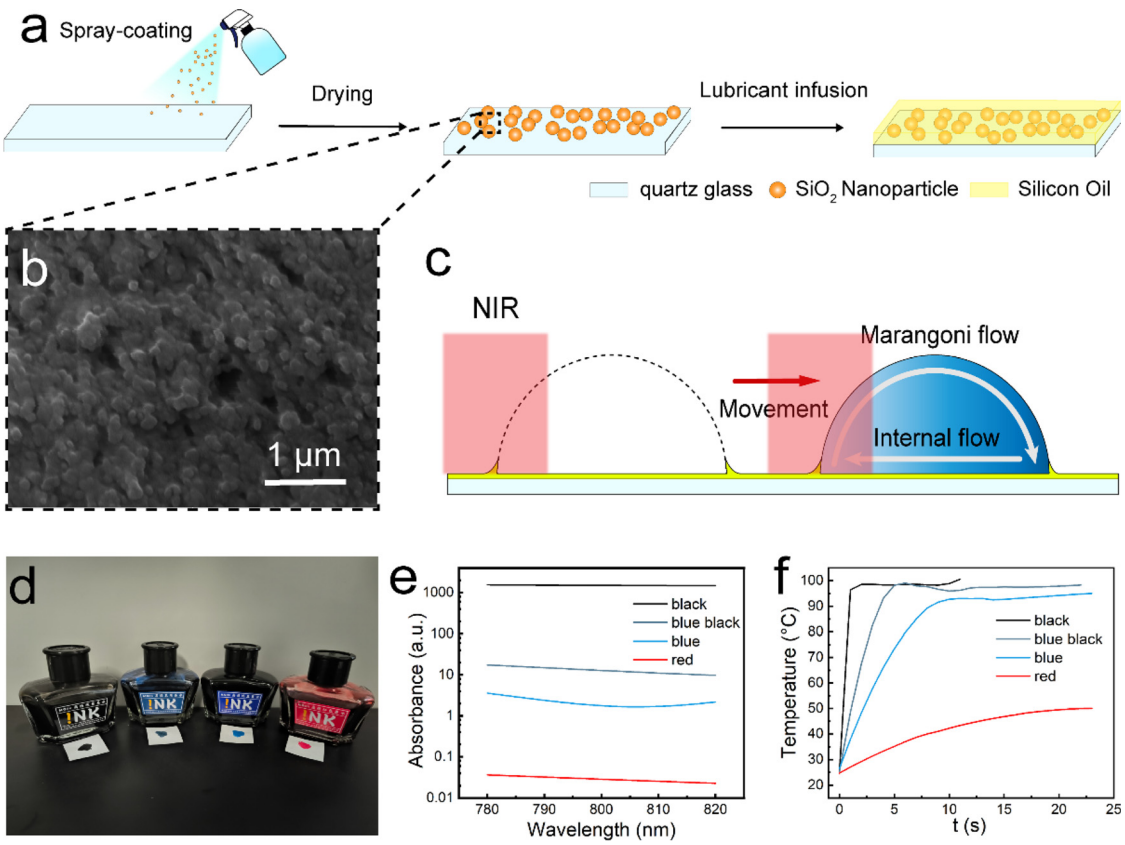

FIG. 1. (a) Cartoon diagram showing the preparation process of the SPSS. (b) The SEM image of the substrate surface before lubricant infusion. (c) Schematic illustration of near-infrared light irradiating one end of an ink droplet to excite a Marangoni flow inside it, driving the droplet forward. (d) Four different colors of ink used in the experiment. (e) Absorbance spectra of four different colored inks. (f) The time-depended temperature profiles of four different colors of ink droplets fixed on the glass sheet under NIR irradiation (808 nm, 1 W).

up to 100 °C in a second or two, while red ink can only reach about 50 °C even after taking ten times longer.

The movement of four ink droplets with different colors but the same volume (15 μl) on SPSS under the NIR irradiation is shown in Fig. 2(a). The four ink droplets start from the same spot. As time continues to increase, the difference in the distance traveled by different color ink droplets increases. If the droplets are arranged according to the movement distance from farthest to nearest, the order is black, blue black, blue, and red, which is consistent with the absorbance order of ink. Figure 2(b) plots the displacements Δx of the four 15 μl ink droplets relative to the starting point over time t. Overall, the displacements of the four ink droplets increase significantly at different speeds. Specifically, the black ink droplet is the fastest, the blue black ink droplet is slightly faster than the blue one, and the red ink droplet is the slowest. But they all show a tendency to change from nonlinear to linear, which means that the movement of the ink droplet goes through two stages. In the first stage, the displacement increases nonlinearly with time, indicating that the ink droplet is undergoing a variable acceleration motion, which can be seen more clearly in the enlarged inset at the lower right corner of Fig. 2(b). After a characteristic time, the ink droplet reaches the second stage, and its displacement begins to increase linearly, indicating that the ink droplet enters the stage of uniform motion. Moreover, the time varying velocities v of the four different color ink droplets are extracted, and the corresponding curves are shown in Fig. 2(c). It is easy to see that the four droplets do go through two phases from accelerated motion to uniform motion.

In addition to the color of the ink droplet, its volume is also an important parameter that affects its movement. Figure 3(a) shows the snapshots of the movement of black ink droplets of five different volumes. All ink droplets start from the same point, and at the 3s moment, the smallest ink droplet is noticeably ahead of the other droplets. It illustrates that the smaller the size of the ink droplet, the faster it moves. As time goes on, the spacing between the droplets of different sizes become larger and larger, demonstrating their difference in velocity of motion. The average accelerations $\bar{a}$ of the four colors and five sizes of ink droplets during the accelerated motion stage, as well as their steady-state velocities V_{st} during the uniform motion stage, are shown in Figs. 3(b) and 3(c), respectively.

It can be seen from Fig. 3(b) that for the same color ink droplets, the average acceleration decreases as the volume of the droplet increases, in which the black ink droplet and blue black one have the most significant changes. For ink droplets with the same size, the smaller the droplet (such as 5 and 10 μl cases), the average acceleration of the droplet decreases faster as the color changes from black to red. However, when the volume increases to a certain extent (for example, above 15 μl), the average acceleration gap between different color ink droplets rapidly decreases. As shown in Fig. 3(c), with the increase in the ink droplet size, the steady velocity of the black, blue black, and blue ink droplets all decreases in different degrees, while the steady velocity of the red ink droplet does not change much. For the same volume of ink droplet, its steady-state velocity varies significantly with the change of ink droplet color. Specifically, the steady velocity of black ink droplet is the largest, followed by the blue black, and blue ink droplets, and the velocity of red ink droplet is the smallest, which is also the same as the results discussed above. Two conclusions can be drawn from Figs. 3(b) and 3(c): the average acceleration and steady velocity of the ink droplet increase with the increase in the absorbance of the droplet, but decrease with the increase in the droplet size. It is worth noting that the second conclusion is contrary to the previous conclusion that the speed of droplets is proportional to their volume.[36] This is because in that work, the temperature gradient is generated on the substrate surface rather than on the droplet, so the larger volume of the droplet means a larger contact radius, and a larger temperature gradient can be obtained, so the droplet moves faster, which is different from the case of direct heating of the ink droplet with near infrared light in this work.

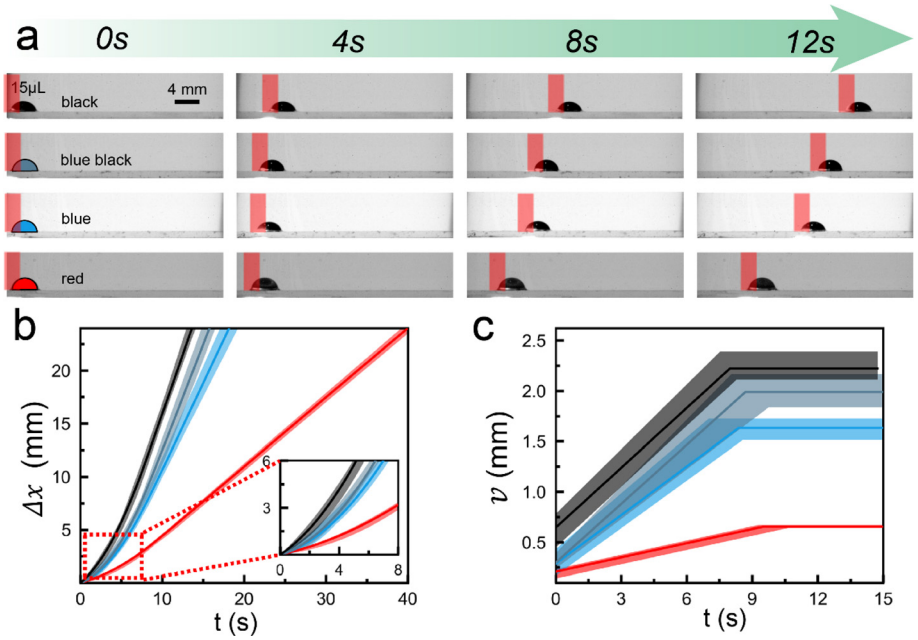

FIG. 2. (a) Snapshots of four ink droplets of the same volume but different colors moving on the surface under the NIR irradiation. All the ink drops appear black is because the high-speed camera used was monochromatic. The color of the droplets at time zero is artificially added to make them easier to distinguish. (b) The plots of the time-depended displacements of the four 15 μl ink droplets. The lower-right inset enlarges the displacements during the variable acceleration stage. The shadows show the error range of the data. (c) The plots of the time-depended velocities of the ink droplets.

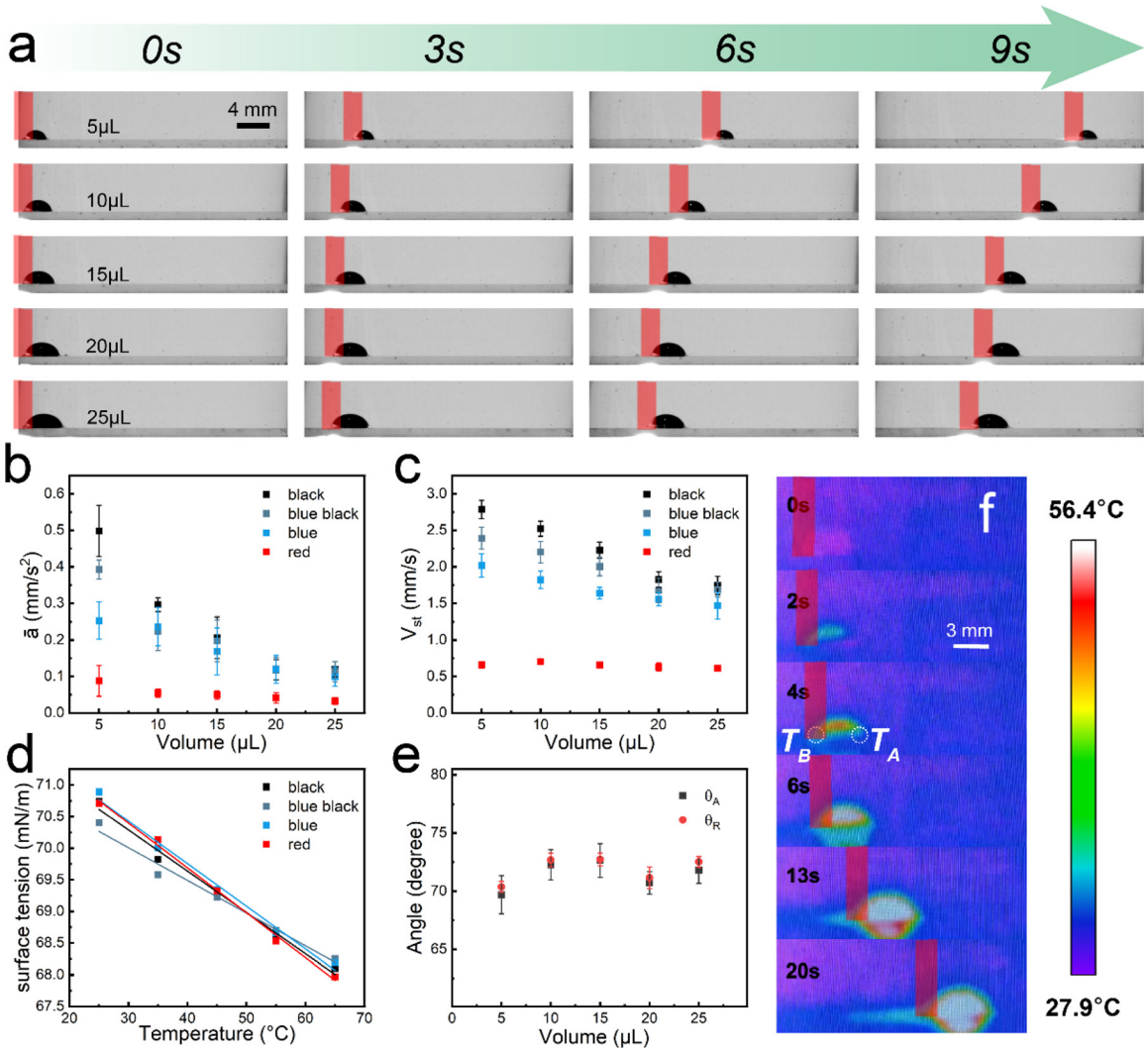

FIG. 3. (a) Snapshots of five black ink droplets with different volumes moving on the surface under the NIR irradiation. (b) Variation of the average acceleration of different color ink droplets with their volume. (c) Variation of the steady velocity of different color ink droplets with their volume. (d) Variation of the surface tension of ink droplets with temperature. (e) Variation of the advancing contact angle and receding contact angles of the black ink droplet with volume. (f) Snapshots of a blue ink droplet (15 μl) taken by an infrared thermal camera.

For droplets on the sliding surface irradiated by near-infrared light, there are two main driving forces to promote their movement. One is the Marangoni force, which arises from the thermocapillary convection inside the droplet as described above, and is proportional to the temperature gradient at the air–liquid interface. Its expression is[36]

$$F_M \approx \pi R^2 \frac{d\gamma_a}{dT}\frac{dT}{dx}, \tag{1}$$

where R is the contact radius of the droplet with the substrate and γ_a is the surface tension of the droplet. Thus, the Marangoni force depends not only on the size of the droplet, but also on the change rate of the surface tension of the droplet with temperature $d\gamma_a/dT$ and the temperature gradient at the two ends of the droplet dT/dx. Figure 3(d) shows the change of the surface tension of four different color ink droplets with the increase in temperature. The absorbance has an effect on the temperature gradient. Specifically, the higher the absorbance of the ink, the faster the temperature of the irradiated end of the droplet rises, the higher the temperature value is reached, and the temperature gradient at both ends of the droplet with the same volume is correspondingly higher. The other driving force is the Laplace force. It is a net surface tension force due to the different contact angles at the two ends of the droplet, which is expressed as[37]

$$F_L = 2R\gamma_a(\cos\theta_A - \cos\theta_R), \tag{2}$$

where θ_A and θ_R are the advancing and receding contact angle of the droplet, respectively. In addition, as the droplet moves forward, it is also subjected to a backward hydrodynamic resistance force caused by

the viscous obstruction of the lubricant and the liquid medium, which could be expressed as[36]

$$F_H \approx \alpha(\mu_o + \mu_l)v\pi R, \tag{3}$$

where α is a numerical factor, μ_o and μ_l are the viscosity of the lubricant oil and liquid, and their values are 0.78 and 1.2 mPa s, respectively. Since the viscous resistance force is proportional to the velocity of the droplet, this can qualitatively explain the two stages of droplet motion observed in the experiment. Under the irradiation of NIR, a stationary ink droplet begins to accelerate. As the speed gradually increases, the resistance increases, the resultant force gradually decreases, and the droplet experiences variable acceleration motion. When the droplet reaches the steady velocity, the hindering force and the driving force are balanced, and the droplet maintains a uniform motion. At the same time, different sizes and different temperature gradients (caused by different heating rates) directly affect the driving force of the ink droplet, which would inevitably affect the acceleration and steady velocity of the droplet. This is also consistent with experimental results.

To further figure out which driving force plays a more important role in the movement of the ink droplet, we carried out a quantitative analysis of the force. Figure 3(e) exhibits the measurement data of the advancing and receding contact angles of the black ink droplet of different sizes in the process of movement. There is little difference between the two contact angles, suggesting that the effect of the Laplace force is so small as to be negligible. Figure 3(f) shows the temperature distribution of a blue ink droplet captured by an infrared thermal camera at different times during its movement. T_A and T_B are the temperatures at the front end (non-light irradiated end) and the tail end (light irradiated end) of the moving droplet, respectively. Taking the fourth second as an example, when the ink droplet has just moved, and the temperature difference between its two ends is $\Delta T = T_B - T_A \approx 3\,^{\circ}\mathrm{C}$. So that such a 15 μl blue ink droplet has a temperature gradient dT/dx of 1.54 K mm^{-1}. Plugging in all the data, we obtain $F_M \approx 0.6$ and $F_H \approx 0.597$ μN, and the corresponding acceleration $a = (F_M - F_H)/m$ is 0.2 mm s^{-2}, where m is the mass of the ink droplet. Then, let $F_M = F_H$, the steady velocity V_{st} of the ink droplet is obtained as 1.5 mm s^{-1}. Here, the value of the numerical factor α is set as 33, which is also close to the reference value mentioned in a previous work.[36] The values of acceleration and steady velocity are in good agreement with the results shown in Figs. 3(b) and 3(c), respectively, which shows that the theoretical model is applicable to this ink droplet-SPSS sliding case.

Through the investigation of previous literature, we find that the manipulation of light-driven droplets in the past was usually limited to the extent of a single droplet,[33] for example the high-fidelity transport of droplets along various paths, which is also easily achieved in our experiment (see Fig. S3 in the supplementary material). However, it is rare to maneuver multiple droplets simultaneously. To this end, we propose a customized transport and merging strategy for multiple ink droplets, as shown in Fig. 4. The first step is to expand the beam spot of the near infrared ray to an appropriate size to cover more ink droplets. This is thanks to the high-power NIR light source, which ensures that there is enough intensity of light irradiated on each droplet. Then, a circular baffle (the shape of the baffle can be adjusted according to demand) is used to the block part of the light spot to form a hollow circle light field, and the four different color ink droplets of the same size

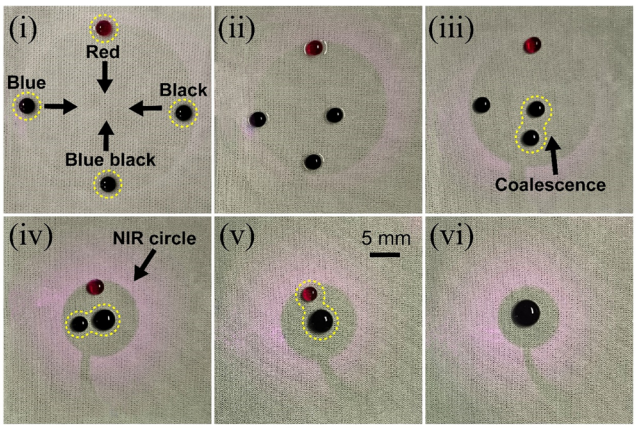

FIG. 4. The demonstration of simultaneous regulation of the transport and merging process of multiple ink droplets using a tunable hollow NIR field. The color differentiation of black, blue black, and blue ink droplets is limited due to shooting conditions.

are located at the boundary of the hollow light field [see Fig. 4(i)]. Stimulated by light irradiation, the ink droplets move toward the center at different speeds, with black moving the fastest and red moving the slowest, as shown in Fig. 4(ii). In this process, the hollow radius of the light field is constantly regulated (which can be achieved by controlling the distance between the baffle and the light source) to ensure that all droplets are within the light control range. At moment (iii–v) of Fig. 4, four colors of ink droplets arrive at the merging center one by one to merge, and finally, all four ink droplets merge into one large droplet, as shown in Fig. 4(vi). In a practical application, the color and size of the ink droplets can be adjusted to achieve the desired merging order. The customized multiple ink droplets transport and merging strategy proposed in this work may have potential applications in droplet-based printing or other areas related to droplet manipulation.

In summary, here we present a method for the precise maneuver of ink droplets via near infrared light-driven on LIS. It is found that the ink droplet would experience two stages from variable acceleration to uniform motion, and the absorbance (color) and size of the ink droplet can affect its motion ability, which is reflected in the difference of the acceleration of the droplet in the acceleration stage and the steady-state velocity in the uniform phase. Our work further reveals that the Marangoni flow inside the ink droplet caused by the temperature gradient at two ends of the droplet under the excitation of light is the main driving force, rather than the Laplace force. We have not only demonstrated that this approach can achieve conventional precise manipulation of individual ink droplets, including robust transport along any path, but also innovatively proposed and validated a customized multiple ink droplets transport and merging strategy. This study may inspire more studies of precise manipulation of light-driven droplets and may find potential applications in droplet-based inkjet printing, textile printing, or other fields related to droplet manipulation.

See the supplementary material for more details of experiments and data analysis, including (1) surface preparation, (2) characterization, (3) the plot of displacement and velocity of ink droplet for varied

color and volume, and (4) demonstration of path manipulation of a single ink droplet.

This research was supported by the Chongqing Human Resources and Social Security Bureau (No. CX2023079), the Fundamental Research Funds for the Central Universities, China (Nos. 2023CDJXY-049 and 2024CDJXY-022), and Wenzhou Key Laboratory of Biophysics (No. WIUCASSWWL22002).

AUTHOR DECLARATIONS

Conflict of Interest

The authors have no conflicts to disclose.

Author Contributions

Yalin Hu: Conceptualization (equal); Data curation (lead); Investigation (lead); Methodology (equal); Validation (lead); Writing – original draft (lead). **Jie Wu:** Methodology (equal); Visualization (equal). **Haiyan Luo:** Investigation (supporting); Visualization (equal). **Guanqi Su:** Data curation (supporting); Investigation (supporting); Visualization (supporting). **Xiangxi Meng:** Investigation (supporting); Methodology (supporting); Visualization (supporting). **Liyu Liu:** Funding acquisition (equal); Supervision (equal). **Guo Chen:** Conceptualization (lead); Funding acquisition (lead); Project administration (lead); Supervision (lead); Writing – review & editing (lead).

DATA AVAILABILITY

The data that support the findings of this study are available from the corresponding author upon reasonable request.

REFERENCES

[1]S. M. Fu, Y. S. Zhou, J. Zhao, K. Pei, and Z. G. Guo, Appl. Mater. Today **40**, 102429 (2024).
[2]C. Farzeena, T. V. Vinay, B. S. Lekshmi, C. M. Ragisha, and S. N. Varanakkottu, Soft Matter **19**, 5223 (2023).
[3]Y. X. Chen, K. Li, S. D. Zhang, L. Qin, S. H. Deng, L. Y. Ge, L. P. Xu, L. L. Ma, S. T. Wang, and X. J. Zhang, ACS Nano **14**(4), 4654 (2020).
[4]Y. M. Zheng, H. Bai, Z. B. Huang, X. L. Tian, F. Q. Nie, Y. Zhao, J. Zhai, and L. Jiang, Nature **463**, 640 (2010).
[5]Y. M. Zheng, X. F. Gao, and L. Jiang, Soft Matter **3**, 178 (2007).
[6]Y. Yang, Q. R. Zou, H. S. Ren, Y. Wang, X. Yao, C. H. Guo, L. J. Zhuo, Y. C. Xu, Y. G. Song, K. F. Xiang, and G. Q. Li, Appl. Phys. Lett. **124**(16), 161902 (2024).
[7]A. K. Kota, G. Kwon, and A. Tuteja, NPG Asia Mater. **6**, e109 (2014).
[8]X. Zeng, Z. G. Guo, and W. M. Liu, Bio-Des. Manuf. **4**, 506 (2021).
[9]J. Li, J. Q. Li, J. Sun, S. L. Feng, and Z. K. Wang, Adv Mater. **31**, 1806501 (2019).
[10]H. Y. Dai, C. Gao, J. H. Sun, C. X. Li, N. Li, L. Wu, Z. C. Dong, and L. Jiang, Adv Mater. **31**, 1905449 (2019).
[11]S. L. Lee, S. G. Lee, H. S. H. S. Hwang, J. R. Hong, S. N. Lee, J. H. Lee, Y. C. Chae, and T. Y. Lee, RSC Adv. **6**, 66729 (2016).
[12]Y. Tang, X. L. Yang, Y. M. Li, and D. Zhu, Adv. Mater. Interfaces **8**, 2100284 (2021).
[13]X. J. Liang, D. K. Li, S. P. Li, J. X. Huang, Z. G. Guo, and W. M. Liu, Chem. Eng. J. **411**, 128464 (2021).
[14]C. L. Gao, L. Wang, Y. C. Lin, J. D. Li, Y. F. Liu, X. Li, S. L. Feng, and Y. M. Zheng, Adv. Funct. Mater. **28**, 1803072 (2018).
[15]Q. Li, D. H. Wu, and Z. G. Guo, Soft Matter **15**, 6803 (2019).
[16]J. Wang, W. Gao, H. Zhang, M. H. Zou, Y. P. Chen, and Y. J. Zhao, Sci. Adv. **4**, eaat7392 (2018).
[17]J. Kamei and H. Yabu, Adv. Funct. Mater. **25**, 4195 (2015).
[18]J. B. Boreyko and C. H. Chen, Phys. Rev. Lett. **103**, 184501 (2009).
[19]K. C. Park, P. S. Kim, A. Grinthal, N. He, D. Fox, J. C. Weaver, and J. Aizenberg, Nature **531**, 78 (2016).
[20]J. Liu, H. Y. Guo, B. Zhang, S. S. Qiao, M. Z. Shao, X. R. Zhang, X. Q. Feng, Q. Y. Li, Y. L. Song, L. Jiang, and J. J. Wang, Angew. Chem., Int. Ed. Engl. **55**, 4265 (2016).
[21]M. He, Y. Ding, J. Chen, and Y. L. Song, ACS Nano **10**, 9456 (2016).
[22]X. M. Chen, J. Wu, R. Y. Ma, M. Hua, N. Koratkar, S. H. Yao, and Z. K. Wang, Adv. Funct. Mater. **21**, 4617 (2011).
[23]R. Malinowski, I. P. Parkin, and G. Volpe, Chem. Soc. Rev. **49**, 7879 (2020).
[24]P. Lv, Y. L. Zhang, D. D. Han, and H. B. Sun, Adv. Mater. Interfaces **8**(12), 2100043 (2021).
[25]Y. B. Peng, C. Z. Li, Y. L. Jiao, S. W. Zhu, Y. L. Hu, W. Xiong, Y. Y. Cao, J. W. Li, and D. Wu, Langmuir **39**(16), 5901 (2023).
[26]S. Ben, T. T. Zhou, H. Ma, J. J. Yao, Y. Z. Ning, D. L. Tian, K. S. Liu, and L. Jiang, Adv. Sci. **6**(17), 1900834 (2019).
[27]K. S. Khalil, S. R. Mahmoudi, N. Abu-dheir, and K. K. Varanasi, Appl. Phys. Lett. **105**(4), 041604 (2014).
[28]M. Abdelgawad and A. R. Wheeler, Adv. Mater. **21**, 920 (2009).
[29]N. Sinn, M. T. Schür, and S. Hardt, Appl. Phys. Lett. **114**(21), 213704 (2019).
[30]G. Kwon, D. Panchanathan, S. R. Mahmoudi, M. A. Gondal, G. H. Mckinley, and K. K. Varanasi, Nat. Commun. **8**, 14968 (2017).
[31]P. Y. Chiou, S. Y. Park, and M. C. Wu, Appl. Phys. Lett. **93**(22), 221110 (2008).
[32]X. Han, S. D. Tan, Q. Wang, X. B. Zuo, L. P. Heng, and L. Jiang, Adv. Mater. **36**, 2402779 (2024).
[33]H. S. Hwang, P. Papadopoulos, S. Fujii, and S. H. Wooh, Adv. Funct. Mater. **32**(15), 2111311 (2022).
[34]T. S. Wong, S. H. Kang, S. K. Y. Tang, E. J. Smythe, B. D. Hatton, A. Grinthal, and J. Aizenberg, Nature **477**, 443 (2011).
[35]Z. T. Hao and W. H. Li, Nanomaterials **11**(3), 801 (2021).
[36]N. Bjelobrk, H. L. Girard, S. B. Subramanyam, H. M. Kwon, D. Quere, and K. K. Varanasi, Phys. Rev. Fluid. **1**, 063902 (2016).
[37]M. K. Chaudhury and G. M. Whitesides, Science **256**, 1539 (1992).